Constraints to the Flat Band Potential of Hematite Photo-electrodes

Journal:	*Physical Chemistry Chemical Physics*
Manuscript ID:	CP-ART-01-2014-000096.R5
Article Type:	Paper
Date Submitted by the Author:	06-Jun-2014
Complete List of Authors:	Hankin, Anna; Imperial College London, Chemical Engineering Alexander, John; Imperial College London, Department of Materials Kelsall, Geoffrey; Imperial College London, Department of Chemical Engineering and Chemical Technology

Physical Chemistry Chemical Physics RSCPublishing

ARTICLE

Constraints to the Flat Band Potential of Hematite Photo-electrodes

Cite this: DOI: 10.1039/xoxxoooooox

A. Hankin,[a] J.C. Alexander[b] and G.H. Kelsall[a]

Received ooth January 2012,
Accepted ooth January 2012

DOI: 10.1039/xoxxoooooox

www.rsc.org/

We revisit the fundamental constraints that apply to flat band potential values at semiconductor photo-electrodes. On the physical scale, the Fermi level energy of a non-degenerate semiconductor at the flat band condition, $E_{F(FB)}$, is constrained to a position between the conduction band, E_C, and the valence band, E_V,: $|E_C| < |E_{F(FB)}| < |E_V|$ throughout the depth of the semiconductor. The same constraint applies on the electrode potential scale, where the values are referenced against a common reference electrode: $U_{C(FB)} < U_{F(FB)} < U_{V(FB)}$. Some experimentally determined flat band potentials appear to lie outside these fundamental boundaries. In order to assess the validity of any determined flat band potential, the boundaries set by the conduction band and the valence band must be computed on both scales *a priori*, where possible. This is accomplished with the aid of an analytical reconstruction of the semiconductor | electrolyte interface in question. To illustrate this approach, we provide a case study based on synthetic hematite, α-Fe_2O_3. The analysis of this particular semiconductor is motivated by the large variance in the flat band potential values reported in the literature.

Introduction

The flat band potential is one of the key parameters that are used in the evaluation of the performance of photo-electrodes when they are employed to drive electrochemical processes, such as water splitting. The extent to which the observed potential of photocurrent onset, whether it is anodic photocurrent at an *n*-type semiconductor or cathodic photocurrent at a *p*-type semiconductor, deviates from the flat band potential serves as one of the measures of the effectiveness of the photo-electrode. Minimal deviation entails the lowest external bias requirements and hence results in the best performance.

The accurate determination of the flat band potential for the specific semiconductor material under investigation is a prerequisite and serves multiple purposes:

1. Demarcation between depletion and accumulation in the semiconductor space charge region;

2. Benchmarking the interfacial photo-generated charge transfer kinetics to aid comparison between different materials;

3. Analysis of the efficiencies of photo-driven processes;

4. Numerical modelling of external bias distribution at the semiconductor | electrolyte interface;

5. Computation of kinetic parameters.

For extrinsic and nano-structured semiconductors, which are presently being developed worldwide for use in energy conversion systems, typically neither the Fermi level energy nor the potential under flat band conditions are known *a priori*. The flat band potential is usually determined experimentally using electrochemical and photo-electrochemical methods when the semiconductor is immersed in the electrolyte solution of interest. Unfortunately, the flat-band potential cannot be measured directly; it is determined indirectly by fitting certain parameters, measurable on the electrode potential scale, to models of the semiconductor | electrolyte interface[1,2,3]. It will be demonstrated in a subsequent communication that some of the popular models that are used to evaluate the flat band potentials on semiconductor electrodes, even in simple electrolytes, are often too simplified to yield reliable flat band potential values and different determination methods may yield different estimates of the flat band potential for the same sample. The application of interfacial models without consideration of the possible deviations from ideal behaviour can result in mis-characterisation.

In order to examine the fundamental plausibility of a measured flat band potential, we start by reiterating a fundamental constraint: with the exception of degenerate, quasi-metallic semiconductors, the potential of a semiconductor at flat band must lie between the potential of the conduction band and the potential of the valence band at the same condition. Hence, when possible, the feasibility of any measured flat band potential value should be ascertained in the first instance by ensuring that this criterion is satisfied.

Unlike the semiconductor potential, U_F, the conduction and valence band positions on the electrode potential scale, U_C and

U_V, are not measureable quantities. However, in principle, at the flat band condition $U_{C(FB)}$ and $U_{V(FB)}$ can be estimated more accurately than $U_{F(FB)}$, so the aim presently is to revisit the method by which this may be accomplished.

The conduction and valence band energies on the physical scale, E_C and E_V, respectively, are calculable for stoichiometric semiconductors using an empirical formula[4]. E_C and E_V will remain constant even when the bands are bent, provided the condition of band edge pinning is satisfied[5]. The subsequent determination of the corresponding values U_C and U_V on the electrode potential scale, under any condition, entails a conversion between the two scales. Such conversion requires an analytical approach and relies on an accurate representation of the semiconductor | electrolyte interface under investigation.

The analytical determination of the potentials of the conduction and valence bands at flat band conditions is illustrated here using hematite, α-Fe_2O_3, as a case study. Synthetic hematite has attracted considerable attention as a photo-anode in photo-electrochemical reactors for solar water splitting[6,7,8]. Theoretically, its band gap of 1.9 - 2.2 eV[9,10,11] enables it to absorb up to ca. 37 - 30 % of solar photons, as determined by integrating the AM 1.5 solar irradiance spectrum (ASTM G173-03 Reference Spectra[†]) with respect to wavelength, λ, for $\lambda \leq \lambda_{\text{band gap}}$.

A selection of flat band potential values reported in the literature for both undoped and doped synthetic hematite electrodes is presented in Table 1. Several preliminary observations can be made about this data sample.

Firstly, the flat band potential values span a range of -0.71 to +0.13 V(SHE). The charge carrier concentrations in the semiconductors employed span the range 3.7×10^{23} – 7×10^{26} m^{-3}; using the explicit theoretical dependence of the semiconductor Fermi level on charge carrier concentration[12] (Equations 25 and 26), we compute that the effect of the reported spread in the charge carrier concentrations on the positions of the Fermi levels in the semiconductors should result in a spread of |0.2| eV (|0.2| V) only. The pH of the electrolytes employed spans the range 13-14.5; this range may be expected to contribute to a spread of |0.09| V in the flat band potential, assuming a Nernstian gradient of 59 mV pH^{-1} in the flat band potential against pH for monovalent ions. Therefore, the additive effect of the spread in charge carrier concentrations and pH accounts for a variation of only |0.3| V in the flat band potential, whereas the spread determined experimentally is almost triple this value.

Furthermore, it will be demonstrated below that a large proportion of the flat band potential values listed in Table 1 appear to lie negative of the potential corresponding to the hematite conduction band edge, seemingly violating the $U_{C(FB)} < U_{F(FB)} < U_{V(FB)}$ criterion.

Authors	Reported Flat Band Potential $U_{F(FB)}^{(Fe_2O_3)}(\text{RE})$ [V]	Electrolyte	Flat Band Potential $U_{F(FB)}^{(Fe_2O_3)}(\text{SHE})$ [V][‡]	Charge Carrier concentration n_0 [m^{-3}]	Method
Horowitz[13]	-0.95 V (SCE)	1 M NaOH	-0.71	1.1×10^{24} (Zr-Fe_2O_3)	Mott-Schottky (1 - 20 kHz)
Benko et al.[14]	-0.85 V (SCE)	1 M NaOH	-0.61	8×10^{25} (Sn-Fe_2O_3)	Mott-Schottky (14.7 Hz)
Glasscock et al.[15]	-0.84 V (SCE)	1 M NaOH	-0.60	1.3×10^{24} (Undoped)	Mott-Schottky (1 - 10 kHz)
Khan and Akikusa [10]	-0.74 V (SCE)	1 M NaOH	-0.50	2.2×10^{26} (Undoped)	Mott-Schottky (0.1 - 1 kHz)
Kennedy and Frese [16]	-0.73 V (SCE)	2 M NaOH	-0.49	2.6×10^{24} (Undoped)	Mott-Schottky (1kHz)
Quinn et al.[17]	-0.67 V (SCE)	2 M NaOH	-0.43	3.7×10^{23} (Undoped)	Mott-Schottky (1 MHz)
Dare-Edwards et al.[18]	-0.5 V (3.5 M Cl^- | AgCl | Ag)	1 M KOH	-0.30	5×10^{24} (TiO_2 doped Fe_2O_3)	Mott-Schottky (unspecified)
Le Formal et al.[19]	+0.53 V ($RHE_{pH=13.6}$)	1 M NaOH	-0.27	7×10^{26} (Si-Fe_2O_3)	Mott-Schottky (10^{-4} – 10^2 kHz)
Butler et al. [20]	-0.32 V (SCE)	1 M NaOH	-0.08	Unspecified (Undoped)	Photocurrent squared [21]
Klahr et al.[22]	-0.07 V ($AgCl\|Ag_{sat}$)	0.1 M KOH	+0.13	4.8×10^{24} (Undoped)	Mott-Schottky (10^{-5} – 10 kHz)
[‡] Conversion performed by the present authors to aid comparison between the reported values					

Table 1: Flat band potentials on synthetic α-Fe_2O_3 and the corresponding experimental conditions reported in the literature.

Both sets of disparities may have one or several common causes, which can include:

a) The presence of deliberately added dopants or naturally occurring defects, which may exert a large effect on the optical and electronic properties of the semiconductors under investigation[23];

b) Differences in the crystallographic orientation;

c) A difference in the pH of zero charge (pH_{pzc}) for the materials, which may be caused by differences in fabrication methods, crystalline orientation, presence of dopants, or disparity in nanostructure. This would cause a difference in the relative adsorption of charged species on the semiconductor surfaces and therefore generate a spread in the measured flat band potentials;

d) The inapplicability of the chosen procedure for determination of the flat band potential for the particular material; for example, a frequency dependence of the electrical permittivity[24,25] or the application of an inappropriate voltage perturbation frequency may impede the correct determination of the space charge capacitance and therefore lead to an erroneous flat band potential and dopant concentration outputs from the Mott-Schottky equation;

e) The pinning of the Fermi level away from flat band by a redox couple or a surface state[5].

This paper focuses on ascertaining analytically the range of fundamentally plausible flat band potentials at a semiconductor by defining explicitly the potentials of the valence band and conduction band edges, also at flat band conditions, and the associated error due to the influence of pH_{pzc}. Therefore, the influence of the methods for determining the flat band potential and the possible effects of Fermi level pinning are beyond the scope of the present study. Furthermore, we restrict the initial discussion to undoped and stoichiometric semiconductors.

We compare our calculations, which are generalised for semiconductors without account for the presence of defects or specific crystallographic orientations, with the results of several *ab initio* studies of band energies on single crystal structures.

In summary, we revisit the general method for *a priori* computation of the conduction and valence band energies of stoichiometric semiconductors and follow their projection to the electrode potential scale with the aid of schematic representations of the semiconductor | electrolyte interface under various conditions. This method is intended to re-enforce some basic guidelines for identifying the feasible ranges of flat band potentials of semiconductors prior to experimental measurements and so should facilitate the elimination of unrealistic values.

Theory

Definition of the Flat Band Potential

The term *flat band* refers to the condition when a semiconductor in contact with another material is not polarized in the interfacial region. At this condition, the conduction and valence bands are referred to as *flat* and no electric field acts on the charge carriers. The flat band condition is a suitable and important reference state relative to which photo-electrochemical kinetics may be assessed. It is also the reference point of zero band bending, which is important in analysing the capacitance of the space charge layer. At potentials other than the flat band potential, an electric field is present at the semiconductor interface and will either drive the photo-generated electrons into the bulk (depletion condition) or to the surface (accumulation condition).

Structure of the Semiconductor | Electrolyte Interface

The position of the Fermi energy level in the semiconductor at the flat band condition, $E_{F(FB)}$, is the same as it is in an isolated semiconductor in vacuum. The flat band potential, $U_{F(FB)}$, is the corresponding value on the electrode potential scale, where it is expressed relative to a reference electrode that has a fixed and known potential relative to vacuum. However, unless the semiconductor is intrinsic and pure, neither the semiconductor Fermi energy level nor the semiconductor potential at the flat band condition is necessarily known accurately *a priori*. On the other hand, the conduction and valence band energies, E_C and E_V, which lie either side of the Fermi energy level are empirically calculable quantities for stoichiometric semiconductors. Hence, in order to predict the feasible range of flat band potential values for a particular semiconductor, conversion of the calculable band energies to the electrode potential scale is necessary.

In principle, conversion of the quantities characterising the semiconductor on the physical scale to the electrode potential scale is straightforward, provided the effect of net charge in the interfacial region arising from net water dipole orientation, chemisorption and net presence of free charges is taken into account[26,27,28]. The effect of charge extends away from the surface of the solid into the electrolyte over the Helmholtz layer[29], comprising the inner Helmholtz plane (IHP), which includes a single layer of water dipoles and any chemisorbed species in direct contact with the electrode surface, and the outer Helmholtz plane (OHP), which includes fully hydrated ionic charges[29]. Any net charge in these two regions will give rise to an electric field and a corresponding potential drop. The total potential drop across the Helmholtz layer, $\Delta\phi_H$, will have the effect of offsetting the vacuum levels of the semiconductor and the bulk electrolyte by $\Delta\phi_H$, so the projected positions of *all* semiconductor energy levels onto the electrode potential scale will be offset by $\Delta\phi_H$ as well.

At the flat band potential of the particular material under investigation, the potential drop in the Helmholtz layer can be neglected only when the composition of the electrolyte corresponds to the pH of zero charge, pH_{pzc}, provided there are no chemisorbed ions and the net dipole orientation in the IHP does not generate a significant potential drop[27]. At pH_{pzc}, the positively and negatively charged species are present in equal quantities in the OHP, such that the net free charge is zero; hence, the potential drop across the Helmholtz layer is also zero. When the pH of the solution is less than pH_{pzc}, the net surface charge is positive at the flat band potential and $\Delta\phi_{H(FB)} > 0$, while at solution pH higher than pH_{pzc}, the net surface charge at the flat band potential is negative and $\Delta\phi_{H(FB)} < 0$.

A further complication arises due to $\Delta\phi_H$ being a function of interfacial bias[30,31,32]. When the interface is biased and the bands are bent: $E_F \neq E_{F(FB)}$ at the interface and $\Delta\phi_H \neq \Delta\phi_{H(FB)}$, so $U_F \neq U_{F(FB)}$, $U_C \neq U_{C(FB)}$ and $U_V \neq U_{V(FB)}$. The potentials corresponding to the energies of the conduction and valence band edges will shift as a function of interfacial bias. However, on the physical scale, E_C and E_V remain constant even when the bands are bent.

Figure 1 shows schematically the structure of an arbitrary semiconductor | electrolyte interfacial junction. The projection of the semiconductor energy levels on the physical scale (in the units of electron volts, eV) to the electrode potential scale in solution, (in the units of volts, V) is presented for three conditions:

a) The semiconductor under the flat band condition, $E_F = E_{F(FB)}$, and with no potential drop in the Helmholtz layer, pH = pH_{pzc}; $\Delta\phi_{H(FB)} = 0$;

b) The semiconductor under the flat band condition, but with a negative potential drop in the Helmholtz layer due to a net negative charge from adsorbed species, pH > pH_{pzc}; $\Delta\phi_{H(FB)} < 0$;

c) The semiconductor under the flat band condition, but with a positive potential drop in the Helmholtz layer due to a net positive charge from adsorbed species, pH < pH_{pzc}; $\Delta\phi_{H(FB)} > 0$.

In these representations as drawn, the vacuum level of the bulk electrolyte is considered to be fixed, so the potential offset, corresponding to $\Delta\phi_{H(FB)}$, is applied to the vacuum level of the semiconductor.

For all the cases in Figure 1, the quantity which is measured against a reference electrode (RE) is the potential U_F(RE) corresponding to the Fermi level energy in the semiconductor. However, accurate determination of U_F(RE) = $U_{F(FB)}$(RE) presents challenges, as evidenced by the data in Table 1.

While U_C(RE) and U_V(RE) are not measureable quantities, their values at flat band conditions are calculable with respect to a chosen reference electrode. $U_{C(FB)}$ and $U_{V(FB)}$ will vary with $\Delta\phi_{H(FB)}$ and pH in the same way as $U_{F(FB)}$, such that the potential differences between $U_{C(FB)}$ and $U_{F(FB)}$ and between $U_{V(FB)}$ and $U_{F(FB)}$ are conserved for all pH.

For the purpose of schematic representation in Figure 1, the Standard Hydrogen Electrode (SHE) is shown as the reference electrode. In practice, other, more practical, reference electrodes are used. The potentials of several common electrodes relative to SHE are shown in Figure 2.

For certain reference electrodes, such as the saturated calomel reference electrode (SCE) or AgCl | Ag, the potential of the reference electrode versus SHE will be invariant with pH and in this case the measured semiconductor flat band potential will vary with $\Delta\phi_{H(FB)}$ only. For other reference electrodes, such as the reversible hydrogen electrode (RHE) or HgO|Hg, the potential of the reference electrode versus SHE will vary with pH and consequently the variation in the flat band potential will be a function of $\Delta\phi_{H(FB)}$ and also of the potential of the reference electrode relative to SHE.

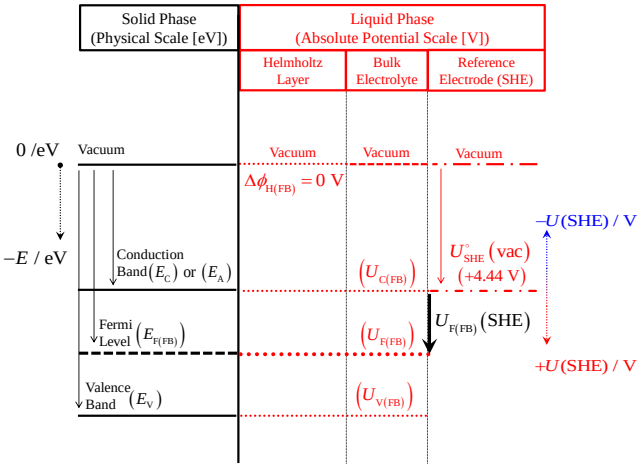

a) Flat band condition, $E_F = E_{F(FB)}$, and at pH_{pzc} ($\Delta\phi_{H(FB)} = 0$ V)

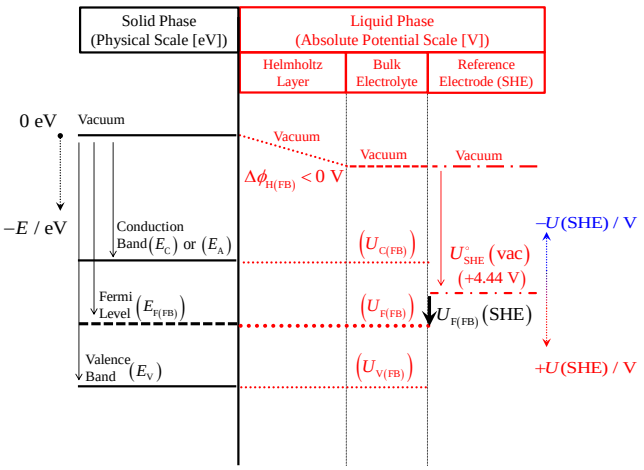

b) Flat band condition, $E_F = E_{F(FB)}$, and at pH > pH_{pzc} ($\Delta\phi_{H(FB)} < 0$ V)

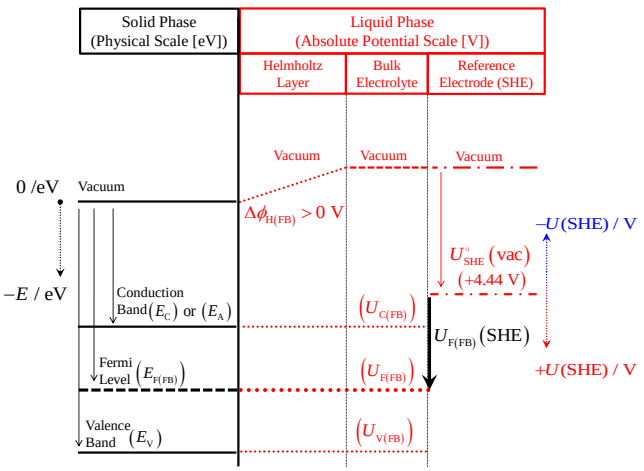

c) Flat band condition, $E_F = E_{F(FB)}$, and at pH < pH_{pzc} ($\Delta\phi_{H(FB)} > 0$ V)

Figure 1: Energy level diagram and corresponding potentials for an arbitrary semiconductor | electrolyte junction.

It should be noted that in all the three cases depicted in Figure 1, the liquid is assumed to be of a sufficiently high ionic conductivity that there is no diffuse double layer, so the potential drop in the solution phase is restricted to the Helmholtz layer. A schematic visualisation of the interface under the conditions of band bending, accompanied by the appropriate interfacial model, is provided elsewhere[33].

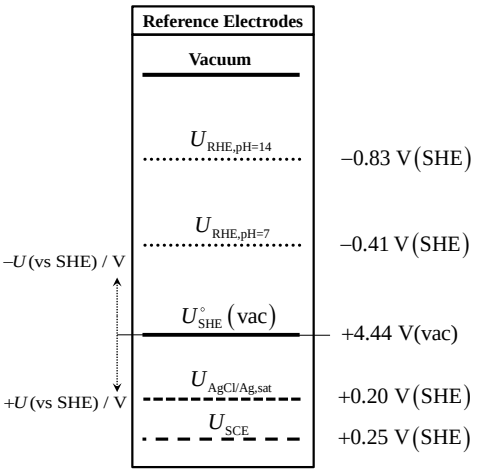

Figure 2: Position of selected reference electrode potentials relative to SHE.

Conversion between the Physical and Electrode Potential Scales

The conversion between quantities defined on the physical scale in the units of electron volts and quantities defined on the absolute potential scale in the units of volts [34], also referred to as the electrode potential scale, is given in Equation 1, below:

$$\text{Physical scale}\,[eV] = -(\text{Absolute potential scale}\,[\text{V}])\times e \qquad (1)$$

Here, the physical scale is assigned the unit of energy: the electron volt [eV], where $1\,[\text{eV}] \cong 1.6\times19^{-19}\,[\text{J}] = 1\,[\text{V}]\times e$. Clearly, when energy is expressed in joules and the relationship between energy and potential is written as $1.6\times19^{-19}\,[\text{J}] = 1\,[\text{V}]\times e$, e is $\approx 1.6\times10^{-19}$ C. However, when writing the relationship as $1\,[\text{eV}] = 1\,[\text{V}]\times e$, e takes the numerical value of unity because the energy is already expressed in terms of a potential acting on an electron.

Equation 1 represents an important difference between the two scales. The physical scale is based on the 'particle in a box' model which applies to an electron bound in a potential well; the energies associated with the discrete energy levels in the well are negative, thereby representing bound particles. The more negative the energy of the electron relative to vacuum, the more strongly it is bound to the nucleus; both the potential and kinetic energies of the electron at vacuum level are zero. The absolute potential scale works in reverse to the physical scale, as the conversion from energy to potential entails division by the electronic charge, which is negative, and so the energy and potential scales move in opposite directions: the more negative the potential, the less negative the corresponding electron energy. Hence, values on the physical scale must always be correctly assigned negative values when introduced into Equation 1. The conversion of energy levels on the physical scale to the electrode potential scale is explained below for the three cases in Figure 1.

For the case in Figure 1(a), when the semiconductor is at flat band and at pH = pH_{pzc}, $E_F = E_{F(FB)}$ and $U_F(\text{SHE}) = U_{F(FB)}(\text{SHE})$ and the potential drop across the Helmholtz layer is zero, $\Delta\phi_{H(FB)} = 0$, the relationship between any energy level (i) in a semiconductor on the physical scale, E_i [eV], and the corresponding value on the electrode potential scale versus the standard hydrogen electrode $U_i(\text{SHE})$ is given in Equation 2[34]:

$$\frac{E_i}{e} = -\left(U_i\,(\text{SHE}) + U^{\circ}_{\text{SHE}}\,(\text{vac})\right) \qquad (2)$$

In which the potential of the SHE versus vacuum at standard conditions [34] is:

$$U^{\circ}_{\text{SHE}}\,(\text{vac}) = U^{o}_{\text{H}^+/\text{H}_2(pH=0)}\,(\text{vac}) = +4.44(\pm0.02)\ \text{V} \qquad (3)$$

and where E_i are negative quantities, by convention, as explained above.

Therefore, the conduction band energy, E_C, usually referred to more formally as the electron affinity, E_A, is converted to the electrode potential scale according to:

$$\frac{E_C}{e} = \frac{E_A}{e} = -\left(U_{C(FB)}\,(\text{SHE}) + U^{\circ}_{\text{SHE}}\,(\text{vac})\right) \qquad (4)$$

where $U_{C(FB)}(\text{SHE})$ is the quantity we wish to compute from a theoretical estimate of E_A.

For the cases in Figure 1(b) and Figure 1(c), for which pH ≠ pH_{pzc} and the potential drop across the Helmholtz layer at flat band, $\Delta\phi_{H(FB)}$, is non-zero, Equation 4 is extended to account for the presence of this potential offset[35]:

$$\frac{E_C}{e} = \frac{E_A}{e} = -\left(U_{C(FB)}\,(\text{SHE}) - \Delta\phi_{H(FB)} + U^{\circ}_{\text{SHE}}\,(\text{vac})\right) \qquad (5)$$

By analogy, the conversion of the valence band energy to the electrode potential scale at flat band is accomplished by

$$\frac{E_V}{e} = -\left(U_{V(FB)}\,(\text{SHE}) - \Delta\phi_{H(FB)} + U^{\circ}_{\text{SHE}}\,(\text{vac})\right) \qquad (6)$$

or simply by

$$U_{V(FB)}\,(\text{SHE}) = U_{C(FB)}\,(\text{SHE}) + \frac{E_G}{e} \qquad (7)$$

where E_G is the band gap of the semiconductor and is a positive quantity.

Finally, when, as in most practical cases, an alternative reference electrode, RE, to SHE is used, Equation 5 is extended to:

$$\frac{E_C}{e} = \frac{E_A}{e} = -\left(U_{C(FB)}\,(\text{RE}) - \Delta\phi_{H(FB)} + U^{o}_{\text{SHE}}\,(\text{vac}) + U\,(\text{RE-SHE})\right) \qquad (8)$$

where $U_{(\mathrm{RE\text{-}SHE})}$ is the potential of the reference electrode relative to SHE.

At flat band potentials, all energies, E_i, refer to both bulk and surface quantities, as by definition they are the same throughout: at the surface and in the bulk. The electrode potentials U_i refer to the measurements made in the bulk electrolyte, where the vacuum level is constant and does not vary with the distance from the electrode surface.

The algorithm for computing the potentials of the conduction and valence bands of stoichiometric semiconductors is summarized in Figure 3.

Equation 5 and Equation 7 will now be applied to compute $U_{C(FB)}$(SHE) and $U_{V(FB)}$(SHE) for α-Fe_2O_3 as a function of pH, and thus provide a bounded range for $U_{F(FB)}$(SHE).

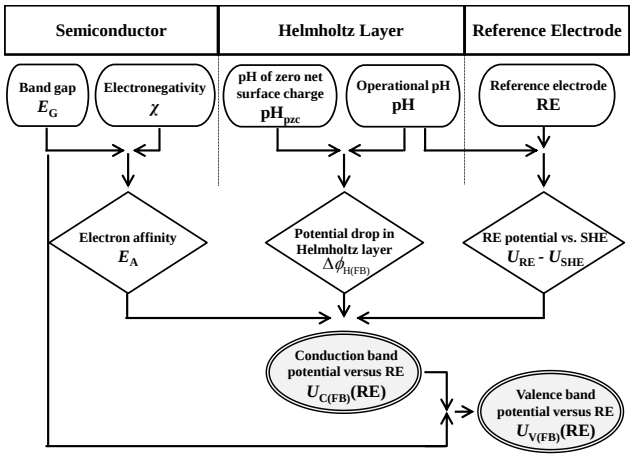

Figure 3: An algorithm aiding the computation of the conduction and valence band potentials of stoichiometric semiconductors at flat band

Interfacial Characterization of Hematite

In order to define the appropriate range of flat band potentials for hematite on the electrode potential scale, i.e. $U_{C(FB)} < U_{F(FB)} < U_{V(FB)}$, the following parameters must be taken into account: the conduction band energy (electron affinity), E_C (E_A), the band gap, E_G, and the potential drop across the Helmholtz layer at flat band, $\Delta\phi_{H(FB)}$, as a function of pH. These parameters will now be considered in turn.

Electron Affinity

The electron affinity of a semiconductor, E_A, is the energy separation between the vacuum level and the bottom of the conduction band; it is a material constant. The electron affinity of a stoichiometric semiconductor compound, such as Fe_2O_3, may be computed empirically from the bulk electronegativity, χ, and the band gap, E_G using an approach proposed by Butler and Ginley[4]:

$$E_A^{(Fe_2O_3)} = -\left|\chi^{(Fe_2O_3)}\right| + \frac{1}{2}E_G^{(Fe_2O_3)} \quad (9)$$

The bulk electronegativity of a compound is the geometric mean of the electronegativities of its constituent atoms[36] and, by analogy with calculations of the conduction band energy of titanium dioxide[4], $E_A^{(TiO_2)}$, and yttrium orthoferrite[20], $E_A^{(YFeO_3)}$, is computed for stoichiometric semiconductors, according to:

$$\chi^{(A_xB_yC_z)} = \left[\chi_{(A)}^{x}\chi_{(B)}^{y}\chi_{(C)}^{z}\right]^{\frac{1}{(x+y+z)}} \quad (10)$$

Therefore, the electronegativity of hematite is determined by:

$$\chi^{(Fe_2O_3)} = \left[\chi_{(Fe)}^{2}\chi_{(O)}^{3}\right]^{\frac{1}{5}} \quad (11)$$

The absolute electronegativity, $\chi^{(j)}$, of an individual atom (j) is computed in units of electron volts, according to Mulliken's definition[37]:

$$\left|\chi^{(j)}\right| = \frac{\left(E_A^{(j)} + I_A^{(j)}\right)}{2} \quad (12)$$

where $E_A^{(j)}$ is the electron affinity and $I_A^{(j)}$ is the ionization energy required to transfer the atom from the neutral state to the singly ionized state. The individual electron affinity, ionization energy and electronegativity values for the iron and the oxygen atoms that form Fe_2O_3 are presented in Table 2.

Quantity [eV]	Fe	O	Reference
$\left\|E_A^{(j)}\right\|$	0.15	1.46	[38]
$\left\|I_A^{(j)}\right\|$	7.90	13.62	[38]
$\left\|\chi^{(Fe_2O_3)}\right\|$	4.03	7.54	Computed from E_A and I_A using Equation 12

Table 2: Electronic properties of iron and oxygen atoms

The bulk electronegativity of iron oxide, $\chi^{(Fe_2O_3)}$, is computed as 5.87 eV, which together with the average value and reported range for the band gap of iron oxide[9,10,11] of 2.05(±0.15) eV gives the electron affinity, $E_A^{(Fe_2O_3)}$, as -4.85(±0.08) eV; this is consistent with previously reported predictions[4,20]. We note that Equation 10 does not take into account the effect of the crystallographic orientation of the material on the electronegativity. The implications of this are addressed in the Discussion section below.

Potential Drop across the Helmholtz Layer

In the absence of specific adsorption, the principal contributions to the overall potential drop across the Helmholtz layer are from the net orientation of water dipoles in the IHP and from the fully hydrated ionic charges in the OHP.

Water dipoles in the IHP may exhibit a net orientation even in the absence of potential drops in the solid or in the OHP; this is

caused principally by chemisorption between the H/O atoms in the dipoles and the surface atoms of the solid[26]. The effect of water dipoles at some metal surfaces have been quantified experimentally and also modelled using the triple-layer model[26,39]: the dipole-induced potential drop may range between several mV to several hundred mV. A similar quantification of the potential drop at oxide semiconductors is considered extremely challenging, in view of the difficulties of data interpretation for such complex interfaces[40]. One set of measurements of the interfacial drop at pH_{pzc} suggests that the dipole contribution could be of order 35(±5) mV[41]. However, it is unclear whether this includes the contribution from band bending and potential differences across electronic connections, so we shall include this value as a contribution to the error in the calculation of the Helmholtz potential drop.

The effect of free charges on the Helmholtz drop becomes important when the operating pH is different from pH_{pzc}. The pH_{pzc} of materials varies greatly with their chemical composition, with the composition of the solution in which they are immersed[17,40,41] and can also exhibit dependence on the structure of the material[42,43], making the prediction of the Helmholtz drop, $\Delta\phi_H$, particularly challenging, even at the flat band potential. In simple electrolytes, such as NaOH or Na_2SO_4, the adsorption of hydroxide ions, OH^-, at pH > pH_{pzc} or hydrogen ions, H^+, at pH < pH_{pzc} will dominate. We have to assume that the surface is pristine and that there is no specific adsorption taking place. It is generally assumed that in the case of monovalent species a Nernstian slope for the potential drop in the Helmholtz layer, $\Delta\phi_H$, at flat band is $\ln(10)RT/F$ (59 mV pH^{-1} at 298.15 K)[44].

However, the slope of 59 mV pH^{-1} and the linearity of the trend in $\Delta\phi_{H(FB)}$ are not always exhibited; some experimental data and models show slopes in $U_{F(FB)}$ of 61 mV pH^{-1} [16], 65 mV pH^{-1} [45] and 73 mV pH^{-1} [16], while a theoretical study shows non-linear trends in $U_{F(FB)}$ with bulk pH[44] which are caused by non-linear trends in $\Delta\phi_{H(FB)}$. Non-linear trends are understood to be a consequence of surface coverage dependent lateral interactions between adsorbed species; in these situations, slopes in $\Delta\phi_H$ as low as 19-38 [41] mV pH^{-1} and 29 [44] mV pH^{-1} have been reported for monovalent species, although the experimental method suggests that the semiconductor was not at the flat band potential during the measurements and hence these slopes are not necessarily relevant to the present discussion.

To allow for a realistic spread in the flat band potential and the conduction and valence band potentials with pH in *a priori* calculations, we neglect the slopes of 38 mV pH^{-1} and below, as well as 73 mV pH^{-1} and above; the former has, to our knowledge, not been reported on hematite while the latter slope is computed from measurements taken outside the stability range of hematite. Hence, a 59±6 mV pH^{-1} slope in $\Delta\phi_{H(FB)}$ is assumed henceforth for monovalent ions.

$$\Delta\phi_{H(FB)}\ [\mathrm{V}] = 0.059(\pm0.006)\{pH_{pzc} - pH\} + \Delta\phi_{dip} \quad (13)$$

A notably wide range of pH_{pzc} has been reported for synthetic polycrystalline and single crystal α-Fe_2O_3 samples, as well as for naturally occurring hematite samples: 6.2─9.5 (6.2[46], 7.0-7.9[40], 7.4[47], 8.0[48], 8.5[49], 8.6[50], 7─9.5[51]). For calculations presented here, an average pH_{pzc} of 7.9(±1.7), based on the aforementioned range, will be used. We add $\Delta\phi_{dip}$ in the form of a (±0.04)V error.

$$\Delta\phi_{H(FB)}^{(Fe_2O_3)} = 0.059(\pm0.006)\{7.9(\pm1.7) - pH\} + (\pm0.04) \quad (14)$$

$$\Delta\phi_{H(FB)}^{(Fe_2O_3)} = 0.47(\pm0.19) - 0.059(\pm0.006)pH \quad (15)$$

with the product error in Equation 15 computed assuming that the Nernstian slope and pH_{pzc} are independent quantities.

We reiterate that Equation 15 is applicable only at flat band potentials. When the potential of the electrode relative to the reference, $U_{applied}$(RE) does not correspond to flat band, $\Delta\phi_H \neq \Delta\phi_{H(FB)}$[30,31,32].

Conduction and Valence Band Potentials

Using:
$E_A^{(Fe_2O_3)}\ [\mathrm{eV}] = -4.85\ (\pm0.08)$,
$U_{SHE}^{\circ}(\mathrm{vac})\ [\mathrm{V}] = +4.44(\pm0.02)$,
$\Delta\phi_{H(FB)}^{(Fe_2O_3)}\ [\mathrm{V}] = 0.47(\pm0.19) - 0.059(\pm0.006)pH$
and SHE as the reference electrode, we compute:

$$\frac{E_A^{(Fe_2O_3)}}{e} = -\left(U_{C(FB)}^{(Fe_2O_3)}(\mathrm{SHE}) - \Delta\phi_{H(FB)}^{(Fe_2O_3)} + U_{SHE}^{\circ}(\mathrm{vac})\right) \quad (16)$$

$$U_{C(FB)}^{(Fe_2O_3)}(\mathrm{SHE}) = -\frac{E_A^{(Fe_2O_3)}}{e} + \Delta\phi_{H(FB)}^{(Fe_2O_3)} - U_{SHE}^{\circ}(\mathrm{vac}) \quad (17)$$

$$U_{C(FB)}^{(Fe_2O_3)}(\mathrm{SHE}) = 0.88(\pm0.29) - 0.059(\pm0.006)pH \quad (18)$$

Of course, further conversions from SHE to a different reference electrode will contain an additional error that depends on how true the value of the reference electrode employed in the experiments is relative to the theoretical value. This is especially important when reference electrodes are employed under the conditions outside their stability range. For instance, $AgCl|Ag_{sat}$ will not be stable in strongly alkaline solutions due to the formation of Ag_2O and AgOH. Also, Hg_2Cl_2(s) in the SCE reference electrode is unstable in alkaline pH[52].

From Equation 18, the potential of the valence band can be determined according to Equation 7, using the band gap value of $E_G^{(Fe_2O_3)}$ = 2.05(±0.15) eV:

$$U_{V(FB)}^{(Fe_2O_3)}(\mathrm{SHE}) = 2.93(\pm0.44) - 0.059(\pm0.006)pH \quad (19)$$

Hematite photo-anodes are employed most commonly in alkaline electrolytes, in particular in 1 M NaOH or 1 M KOH solutions. Such solutions have a pH of approximately 13.7, at which $U_{C(FB)}^{(Fe_2O_3)}(\mathrm{SHE})$ is 0.07(±0.30) V and $U_{V(FB)}^{(Fe_2O_3)}(\mathrm{SHE})$ = 2.12(±0.45) V, so according to the empirical derivation, the flat band potential at that pH should lie between these values.

Discussion

In spite of the generous assignment of errors in the parameters used to derive the expressions for the conduction and valence band potentials on hematite, these predicted boundaries for the flat band potential agree with only two values of the flat band potential[20,22] reported for un-doped hematite in Table 1. In particular, we note that Klahr et al.[22] employ a rigorous approach for the determination of the flat band by applying the Mott-Schottky equation to the interfacial capacitance, extracted by fitting an equivalent circuit to impedance data collected over a range of potentials.

We also duly note that our predictions do not apply to the doped iron oxide electrodes employed to generate the results in Table 1. The presence of foreign interstitial atoms will modify the electronic and optical properties of semiconductors[23]. Furthermore, the pH_{pzc} of doped semiconductors may differ from that of undoped semiconductors. For instance, evidence suggests that pH_{pzc} of hematite may decrease by several units in the presence of silicon[53], which will have the effect of shifting the flat band potential to more negative values. $pH_{pzc}(SiO_2) \approx 2$[54], so high Si surface concentrations would be expected to decrease the pH_{pzc} of Fe_2O_3.

It is conceivable that the empirical formula in Equation 9, which was used for the computation of the electron affinity of stoichiometric semiconductors, is too simplistic. The formula assumes that the electronegativity corresponds precisely to the band gap centre relative to vacuum. In practice, the electronic structure is likely to be affected by the presence of impurities and defects due to the differences in the physical structure arising from varied preparation methods, which included sputtering[11,14], spray pyrolysis[10], chemical vapour deposition[13,19] and atomic layer deposition[19,22] of hematite films and bulk pellets[16,18].

In particular, the effect of crystallographic orientation on the electronic structure of the material is not taken into account in Equation 10. Several reports[55,56] present *ab initio* calculations of the conduction band minimum, valence band maximum and band gap energies in hematite with different crystallographic orientations.

One theoretical study[55] examined the effect of ten crystallographic orientations on the electronic structure of hematite at temperatures both below and above the Morin transition temperature[††]. In the absence of doping, E_G was computed to be 2.04 eV and E_C and E_V are ca. -4.9 eV and -6.9 eV, respectively. It was not apparent which crystallographic plane(s) these calculations correspond to. However, the values of E_C, E_V and E_G are in good agreement with the value computed using Equation 9.

Another study[56] demonstrated that the centre of the band gap relative to vacuum can vary significantly from one crystallographic direction to another. For example, the centres of the band gap for the (0001) and $(01\bar{1}2)$ orientations were computed at -4.48 eV and -5.34 eV, respectively, using density functional theory (DFT+U). Both crystallographic structures have also been shown to occur experimentally[57]. Band positions were then computed from the band gap energy centres using Equation 9; the value of the band gap energy for hematite used in these calculations was 3.08 eV[56], which appears extraordinarily high. If we re-compute the conduction and valence band energies using a band gap of 2.05 eV, E_C/E_V are -3.46/-5.51 eV for the (0001) structure and -4.32/-6.37 eV for the $(01\bar{1}2)$ structure.

However, it is highly unlikely that the energy of the conduction band edge of hematite can lie at -3.46 eV which may be represented on the electrode potential scale as:

$$\frac{-3.46^{(Fe_2O_3)}\ [\mathrm{eV}]}{e} \Rightarrow \{-0.51(\pm 0.17) - 0.059(\pm 0.006)\mathrm{pH}\}(\mathrm{SHE})\ [\mathrm{V}] \quad (20)$$

This potential of the hematite conduction band edge would be negative of the redox energy for water reduction to hydrogen (at all pH), which would imply that spontaneous photo-reduction of water on hematite is possible, though not detected experimentally:

$$2H^+ + 2e^- \rightleftharpoons H_2 \quad (21)$$

$$U^{\circ}_{(H^+/H_2)}(\mathrm{SHE})\ [\mathrm{V}] = -0.059\mathrm{pH} \quad (22)$$

Those potentials would also be negative of the potentials for reduction of hematite to magnetite, suggesting that reaction could be driven spontaneously by photo-generated electrons:

$$3Fe_2O_3 + 2H^+ + 2e^- \rightleftharpoons 2Fe_3O_4 + H_2O \quad (23)$$

$$U^{\circ}_{(Fe_2O_3/Fe_3O_4)}(\mathrm{SHE})\ [\mathrm{V}] = 0.19 - 0.059\mathrm{pH} \quad (24)$$

Both equilibrium potentials were computed from thermodynamic data[58].

Therefore, a value of -3.46 eV for the conduction band edge energy of hematite seems improbable. Conversely, this may suggest that the (0001) surface is electrochemically inactive despite having potentially favourable energetics.

The conduction band position at -4.32 eV[56] for the $(01\bar{1}2)$ planes, agrees better than -3.46 eV with experimental data as evidenced in

Figure 4, which shows the flat band potential data from Table 1, as a function of pH and superimposed on a set of band potentials, obtained using the methods outlined above.

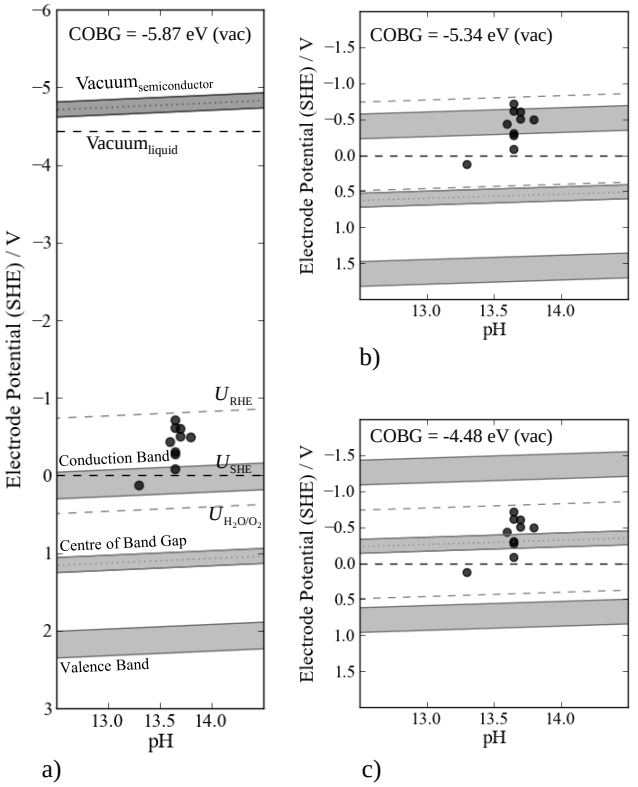

Figure 4: Comparison of the experimental flat band data (solid circles) with calculated values for a range of estimates for the centre of the band gap (COBG) of a) -5.87 eV[this paper, 55], b) -5.34 eV[56], and c) -4.48 eV[56] relative to vacuum. The vacuum level of the semiconductor relative to SHE is shown for the range of pH_{pzc} reported. This results in a range for the COBG relative to SHE. The positions of the conduction and valence bands are then shown based on the reported experimental range of the band gap. Average values are shown with a dotted line while shading represents the range of calculated values. The vacuum level against SHE as well as the reversible potentials for water reduction and oxidation are shown as dashed lines. Panel a) shows the full diagram. Panels b) and c) are restricted to show only the conduction and valence bands.

There is clearly a large uncertainty among the electron affinities computed *ab initio*[55, 56]. An additional complexity that has not been fully discussed is that the band gap, the electron affinity and the pH_{pzc} have all been assumed to be independent of one another and applied as averages in the preceding calculations.

In order to examine which electron affinities (conduction band energies) are realistic, we derive, using Equations 25 and 26, the conduction band energies of the undoped hematite samples presented in Table 1 from the reported flat band potentials. In order to do this, we compute the separation between the Fermi level and the conduction band for each set of data. The potential of the conduction band $U_{C(FB)}^{(Fe_2O_3)}(SHE)$ is calculated by adding ΔE_F to the measured flat band potential, and the electron affinity is calculated using Equation 16; the results are presented in Table 3. The energy separation between the Fermi level and the conduction band at its flat band potential can be computed if the density of states in the conduction band, N_C, and the charge carrier density (electron density) under this condition, n_0, are known[12]:

$$\left(E_{F(FB)} - E_C\right) = k_B T \ln\left\{\frac{n_0}{N_C}\right\} \quad (25)$$

where N_C is a function of the effective mass of the electron in the crystal lattice:

$$N_C = \frac{1}{\sqrt{2}}\left(\frac{m_e^* k_B T}{\pi\hbar^2}\right)^{\frac{3}{2}} \quad (26)$$

In Table 3, we present two conduction band energies for each flat band potential value that were computed using two reported effective electronic masses in hematite, $m_e^* = 1.5m_e$[59] and $2.85m_e$[55(††)]. It appears that only one set of electron affinities[22] determined from the experimental data is in agreement with the empirically determined value of -4.85(±0.08) eV and the value of -4.9 eV computed *ab initio*[55]. Another set of electron affinities is moderately congruent with the conduction band energy of -4.32 eV; this $E_{C(FB)}^{(Fe_2O_3)}$ was determined from the band gap centre of a $(01\bar{1}2)$ hematite crystal[56] and a band gap value of 2.05 eV.

Whether it is correct to compare the conduction band energies of a random set of hematite samples with those of particular crystalline structures remains to be ascertained. However, the incongruity of the experimentally determined and computed flat band potential data may be an indication that individual specimens reported in the literature are composed of grains exposing different crystallographic facets (or ratios thereof) to the electrolyte. More accurate calculations of the band energies may be used to identify and to tune the nanostructure of hematite electrodes to favour a particular crystal facet that has a more negative flat band potential and thus a lower bias for water splitting. While theoretical calculations show the effect of the crystal facet on the position of the centre of the band gap, it is presently unclear what the combined effect each facet has on the band gap, electron affinity, and the pH_{pzc}, all of which affect the position of the flat band potential.

Three remaining entries lie positive of both sets of reported electron affinities: so we are inclined to believe that there is greater accuracy in the more positive $E_{F(FB)}^{(Fe_2O_3)}$ values reported for undoped hematite.

‡ pH unspecified in[15]; value of 13.7 assumed by current authors
‡‡ pH given as 14 in [10], however this is likely to be a theoretical assumption rather than a measurement; hence, a value of 13.7 assumed by current authors
‡‡‡ Both data sets suggest extremely high degeneracy

						Calculations using $m_e^* = 1.5m_e$		Calculations using $m_e^* = 2.85m_e$	
						$N_C = 4.6\times10^{25}$ [m^{-3}]		$N_C = 1.2\times10^{26}$ [m^{-3}]	
Ref.	$U_{F(FB)}^{(Fe_2O_3)}$ (SHE) [V]	pH	$\Delta\phi_{H(FB)}$ [V]	$E_{F(FB)}^{(Fe_2O_3)}$ [eV]	n_0 [m^{-3}]	$E_{F(FB)} - E_C$ [eV]	E_A [eV]	$E_{F(FB)} - E_C$ [eV]	E_A [eV]
15	-0.60	13.7‡	-0.34	-4.18	1.3×10^{24}	-0.092	-4.09	-0.116	-4.06
10	-0.50	13.7‡‡	-0.34	-4.28	2.2×10^{26}	+0.040‡‡‡	-4.32	+0.016‡‡‡	-4.30
16	-0.49	13.8	-0.34	-4.29	2.6×10^{24}	-0.074	-4.22	-0.098	-4.19
17	-0.43	13.6	-0.33	-4.34	3.7×10^{23}	-0.124	-4.22	-0.149	-4.19
22	+0.13	13.3	-0.31	-4.88	4.8×10^{24}	-0.058	-4.82	-0.083	-4.80

Table 3: Computed conduction band energies of several undoped hematite samples presented in the literature

In a final remark on the disparities in the reported flat band potential, we believe it is not unreasonable to suppose that the Mott-Schottky equation is sometimes applied to capacitance values that do not correspond to the semiconductor space charge layer only. This may be responsible for the wide spread and for some of the more negative flat band potentials on hematite presented in Table 1. Some of the suppositions made in the Mott-Schottky analysis[30] are that the interface is perfectly planar, there is no frequency dependence in the intercept of the Mott-Schottky plot with the potential axis and that there is no Fermi level pinning, to name but few; therefore, on nanostructured materials these criteria are not necessarily met.

At the flat band potential, surface states and Fermi Level pinning do not affect the analytical model. However, during experimental determination of the capacitance (and hence the flat band potential), these will affect both the capacitance and the degree of band bending with electrode potential. The Fermi level may be pinned by states localised in the semiconductor band gap or by redox couples whose electrode potential can lie both within and outside the band gaps[60,61]. In these cases, any bias applied across the semiconductor | electrolyte interface affects principally the electrolyte side and hence the potential drop in the Helmholtz layer is different to that predicted for the flat band condition. Fermi level pinning by surface states may be tested with the aid of impedance spectroscopy[22] and also by comparing Mott-Schottky plots in the presence of different redox couples[61]. However, we note that given the similar composition of the electrolytes employed to generate the results in Table 1, if any Fermi level pinning existed due to a common redox couple, the spread in the flat band potentials ought to have been much smaller.

The flat band potential is often obtained by extrapolation of data in Mott-Schottky by over 0.4 V[10,17] or extrapolation of non-linear data trends[18]. This issue is explored in a future publication. Furthermore, the reference electrodes employed to carry out the measurements reported in Table 1 were not necessarily suitable to the conditions to which they were exposed.

Following *a priori* computation of the conduction and valence band potential, in principle, certain parameters used in the computation can be verified experimentally in order to decrease the calculation error. Semiconductor band gaps may be obtained experimentally by UV-visible spectroscopy. The valence band energy of a semiconductor may be determined by ultraviolet photoemission spectroscopy (UPS)[62], while the Fermi level can be determined by a measurement of the work function. Measurements of the band gap and valence band energy should enable the calculation of a semiconductor's electron affinity. The pH_{pzc} of a material may be measured by mass titration[63] or by potentiometric titration[48]. However, the measurement of pH_{pzc} is typically made with powdered samples rather than films. As such, it is rare for the pH_{pzc} of a thin film sample to be known explicitly, though in principle, it could be measured by electrokinetic experiments.

Conclusions

We have revisited the widely accepted empirical method for the computation of the conduction and valence band energies of stoichiometric semiconductors and the analytical method for the conversion of these quantities to the electrode potential scale. The method described is intended to re-enforce the guidelines for identifying the feasible range of flat band potentials of stoichiometric and non-degenerate semiconductors: at flat band the electrode potential must lie between the conduction and valence band potentials.

We compute the conduction and valence band potentials of undoped hematite as

$$U_{C(FB)}^{(Fe_2O_3)}(\mathrm{SHE})\ [\mathrm{V}] = 0.88(\pm0.29) - 0.059(\pm0.006)\,\mathrm{pH}$$

and

$$U_{\mathrm{V(FB)}}^{(\mathrm{Fe_2O_3})}(\mathrm{SHE})\ [\mathrm{V}] = 2.93(\pm 0.44) - 0.059(\pm 0.006)\mathrm{pH},$$

respectively. In these equations, the adsorption of species other than protons and hydroxide ions is neglected. Analysis of flat band data from ten publications shows that more often than not, the flat band values lie outside of these boundaries. There are two possible reasons for this: the calculations do not reflect the hematite bulk / surface structure or the chosen flat band determination method is not always appropriate. Recent *ab initio* calculations of band energies of hematite account for different material structures and so allow for a broader range in flat band potentials. However, a large proportion of reported flat band potentials still remain unexplained and it is possible that this is a consequence of the method used for their determination.

Nomenclature

Symbol	Definition	Unit
E	Energy	eV (throughout document except in Equation (25), where the unit of energy is J)
e	Electronic charge	C
F	Faraday constant	C mol^{-1}
I	Ionisation energy	eV
k_B	Boltzmann constant	J K^{-1}
m	Mass	kg
n or N	Number density	m^{-3}
R	Universal gas constant	J mol^{-1} K^{-1}
T	Temperature	K
U	Electrode potential vs. reference	V
$\Delta\phi$	Potential drop	V (electrode potential scale)
χ	Electronegativity	eV
$\hbar$	Reduced Planck constant	J s

Abbreviation	Definition
RE	Reference Electrode
SHE	Standard Hydrogen Electrode
RHE	Reversible Hydrogen Electrode
SCE	Saturated Calomel Electrode
AgCl|Ag	Silver chloride | Silver Reference Electrode

Subscript / superscript	Definition
C	Conduction band
V	Valence band
F	Fermi level
FB	Value which corresponds to the flat band condition
G	Band gap
H	Quantity characterising the Helmholtz layer
SC	Quantity characterising the semiconductor
pzc	Point of zero charge
vac	Vacuum
e	Electron
*	Effective quantity

Acknowledgements
The authors thank the UK Engineering and Physical Research Council for providing grants, supporting the PDRA position of A.H. and the studentship of J.C.A.

Notes and references
[a] Department of Chemical Engineering, Imperial College London, South Kensington, London SW7 2AZ, UK
[b] Department of Materials, Imperial College London, South Kensington, London SW7 2AZ, UK

† www.nrel.gov/rredc
†† All our comparisons and calculations are made with the $m_e^* = 2.85m_e$ effective mass of electrons in hematite, which corresponds to the (0001) direction with the highest electronic conductivity. For the $(01\bar{1}2)$ direction the effective mass is higher at 13.86 m^0; we also assume that hematite samples used in the published studies will have undergone the Morin transition, a magnetic phase (spin-flop) transition which takes place at $T > T_M$. T_M for hematite is 241 - 261 K[64].

Keywords: ●*flat band potential* ●*semiconductor* ●*hematite* ●*iron oxide*

1 W.J. Albery, G.J. O'Shea and A.L. Smith, *J. Chem. Soc., Faraday Trans.*, 1996, **92**, 4083
2 S.P. Harrington and T.M. Devine, *J. Electrochem. Soc.*, 2008, **155**, C381
3 F. Fabregat-Santiago, G. Garcia-Belmonte, J. Bisquert, P. Bogdanoff and A. Zabanc, *J. Electrochem. Soc.*, 2003, **150**, E293
4 M.A. Butler and D.S. Ginley, *J. Electrochem. Soc.*, 1978, **125**, 228
5 A.J. Bard, A.B. Bocarsly, F.-R.F. Fan, E.G. Walton and M.S. Wrighton, *J. Am. Chem. Soc.*, 1980, **102**, 3671
6 C.K. Ong, S. Dennison, S. Fearn, K. Hellgardt and G.H. Kelsall, Electrochim. Acta, 2014, **125**, 266
7 C. Carver, Z. Ulissi, C.K. Ong, S. Dennison, G.H. Kelsall and K. Hellgardt, *Int. J. Hydrogen Energ.*, 2012, **37**, 2911
8 C.K. Ong, S. Dennison, K. Hellgardt, and G. Kelsall, *ECS Trans.*, 2011, **35**, 11
9 A.A. Akl, *Appl. Surf. Sci.*, 2004, **233**, 307
10 S.U.M. Khan and J. Akikusa, *J. Phys. Chem. B*, 1999, **103**, 7184
11 J.A. Glasscock, P.R.F. Barnes, I.C. Plumb, A. Bendavid and P.J. Martin, *Thin Solid Films*, 2008, **516**, 1716
12 Semiconductor Photoelectrochemistry, Yu.V. Pleskov and Yu.Ya. Gurevich, Consultants Bureau, New York, 1986
13 G. Horowitz, J. Electroanal. Chem., 1983, **159**, 421
14 F.A. Benko, J. Longo and F.P. Koffyberg, *J. Electrochem. Soc.*, 1985, **132**, 609
15 J.A. Glasscock, P.R.F. Barnes, I.C. Plumb and N. Savvides, *J. Phys. Chem. C*, 111 (2007) 16477
16 J.H. Kennedy and K.W. Frese, Jr., *J. Electrochem. Soc.*, 1978, **125**, 723
17 R.K. Quinn, R.D. Nasby and R.J. Baughman, *Mater. Res. Bull.*, 1976, **11**, 1011
18 M.P. Dare-Edwards, J.B. Goodenough, A. Hamnett and P.R. Travellick, *J. Chem. Soc., Faraday Trans. 1*, 1983, **79**, 2027
19 F. Le Formal, N. Tétreault, M. Cornuz, T. Moehl, M. Grätzel and K. Sivula, *Chem. Sci.*, 2011, **2**, 737

20 M.A. Butler, D.S. Ginley and M. Eibschutz, *J. Appl. Phys.*, 1977, **48**, 3070
21 M.A. Butler, *J. Appl. Phys.*, 1977, **48**, 1914
22 B. Klahr, S. Gimenez, F. Fabregat-Santiago, T. Hamann and J. Bisquert, *J. Am. Chem.Soc.*, 2012, **134**, 4294
23 C.E. Cava, L.S. Roman and C. Persson, *Phys. Rev. B*, 2013, **88**, 045136
24 F. Cardon and W.P. Gomes, *J. Phys. D: Appl. Phys*., 1978, **11**, L63
25 K.S.Yun, S.M. Wilhelm, S. Kapusta and N. Hackerman, *J. Electrochem. Soc*., 1980, **127**, 85
26 S. Trasatti, *J. Electroanal. Chem.*, 1975, **64**, 128
27 Surface Electrochemistry, A Molecular Approach, J. O'M. Bockris and S.U.M. Khan, Plenum Press, New York, 1993
28 The Chemical Physics of Surfaces, 2nd ed., S.R. Morrison, Plenum Press, New York, 1977
29 Modern Electrochemistry 2A, 2nd edition, Fundamentals of Electrodics, J. O'M. Bockris, A.K.N. Reddy and M. Gamboa-Aldeco, Kluwer Academic/Plenum Publishers, New York, 2000
30 R. De Gryse, W.P. Gomes, F. Cardon and J. Vennik, *J. Electrochem. Soc*., 1975, **122**, 711
31 J.-N. Chazalviel, *J. Electrochem. Soc.*, 1982, **129**, 963
32 K. Uosaki and H. Kita, *J. Electrochem. Soc.*, 1983, **130**, 895
33 J. Bisquert, P. Cendula, L. Bertoluzzi and S. Gimenez, *J. Phys. Chem. Lett*, 2014, **5**, 205
34 S. Trasatti, *Pure & Appl. Chem.*, 1986, **58**, 955
35 A.J. Nozik, *Ann. Rev. Phys. Chem.*, 1978, **29**, 189
36 A.H. Nethercot, Jr., *Phys. Rev. Lett.*, 1974, **33**, 1088
37 R.S. Mulliken, *J. Chem. Phys.*, 1934, **2**, 782
38 CRC Handbook of Chemistry and Physics, 93rd ed., W.M. Haynes, CRC press, Taylor & Francis Group, London, 2012
39 J. O'M Bockris and M.A. Habib, *Electrochim. Acta*, 1977, **22**, 41
40 P. Hesleitner, D. Babić, N. Kallay and E. Matjević, *Langmuir*, 1987, **3**, 815
41 N. Kallay and T. Preočanin, *J. Colloid. Interf. Sci.*, 2008, **318**, 290
42 R. Parsons, *Chem. Rev*., 1990, **90**, 813
43 Y.T. He, J. Wan and T. Tokunaga *J. Nanopart. Res.*, 2008, **10**, 321
44 S. Licht and V. Marcu, *J. Electroanal. Chem.*, 1986, **210**, 197
45 H. Gerischer, *Electrochim. Acta*, 1989, **34**, 1005
46 S. Mustafa, S. Tasleem and A. Naeem, *J. Colloid. Interf. Sci.*, 2004, **275**, 523
47 Z. Zhang, C. Boxall and G.H. Kelsall, *Colloid Surface A*, 1993, **73**, 145
48 P. Zarzycki, S. Chatman, T. Preočanin, and K. M. Rosso, *Langmuir*, 2011, **27**, 7986
49 M. Gunnarsson, A.-M. Jakobsson, S. Ekberg, Y. Albinsson and E. Ahlberg, *J. Colloid Interf. Sci.*, 2000, **231**, 326
50 R.J. Atkinson, A.M. Posner and J.P. Quirk, *J. Phys. Chem.*, 1967, **71**, 550
51 The Iron Oxides: Structure, Properties, Reactions, Occurrence and Uses, R.M. Cornell and U. Schwertmann, Weinheim, Cambridge: VCH, 1996
52 N.P. Brandon, P.A. Francis, J. Jeffrey, G.H. Kelsall and Q. Yin, *J. Electroanal. Chem.*, 2001, **497**, 18
53 P.R. Anderson and M.M. Benjamin, *Environ. Sci. Technol.*, 1985, **79**, 1048
54 G.A. Parks, *Chem. Rev*., 1965, **65**, 177
55 X. Meng, G. Qin, W.A. Goddard, III, S. Li, H. Pan, X. Wen, Y. Qin and L. Zuo, *J. Phys. Chem. C*, 2013, **117**, 3779
56 M.C. Toroker, D.K. Kanan, N. Alidoust, L.Y. Isseroff, P. Liao and E.A. Carter, *Phys. Chem. Chem. Phys.*, 2011, **13**, 16644
57 A. Shchukarev and J.-F. Boily, *Surf. Interface Anal*., 2008, **40**, 349
58 Standard Potentials in Aqueous Solution, A. Bard, R. Parsons and J. Jordan, Marcel Dekker, New York, 1985
59 H. Peng, S. Lany, *Phys. Rev. B*, 2012, **85**, 201202-1.
60 A.J. Bard, A.B. Bocarsly, F.-R.F. Fan, E.G. Walton and M.S. Wrighton, J. Am. Chem. Soc., 1980, 102, 3671
61 G. Nagasubramanian, B.L. Wheeler, and A.J. Bard, J. Electrochem. Soc., 1983, 130, 1680
62 W.-J. Chun, A. Ishikawa, H. Fujisawa, T. Takata, J.N. Kondo, M. Hara, M. Kawai, Y. Matsumoto and K. Domen, *J. Phys. Chem. B*, 2003, **107**, 1798
63 T. Preočanin and N. Kallay, *Croat. Chem. Acta*, 2006, **79**, 95
64 Ö. Özdemir, D.J. Dunlop and T.S. Berquo, *Geochem. Geophys. Geosyst.*, 2008, **9**, Q10Z01

Manuscript Title: Constraints to the Flat Band Potential of Hematite Photo-electrodes

Manuscript Authors: A. Hankin, J.C. Alexander and G.H. Kelsall

Colour Graphic: N/A

Text: Reasons are discussed for the widely disparate, reported flat band potentials for semiconducting hematite (photo-)electrodes in aqueous solutions